Flame-retardant thermoplastics derived from plant cell wall polymers by single ionic liquid substitution

著者	Nishita Ryunosuke, Kuroda Kosuke, Ota Shohei, Endo Takatsugu, Suzuki Shiori, Ninomiya Kazuaki, Takahashi Kenji
著者別表示	黒田 浩介, 仁宮 一章 , ?橋 憲司
journal or publication title	New Journal of Chemistry
volume	43
number	5
page range	2057-2064
year	2019-03
URL	http://doi.org/10.24517/00056097

doi: 10.1039/C8NJ04797A

Electronic Supplementary Information

Fire-retardant thermoplastics derived from plant cell wall by single ionic liquid substitution

Ryunosuke Nishita, Kosuke Kuroda, Shohei Ota, Takatsugu Endo, Shiori Suzuki,

Kazuaki Ninomiya, and Kenji Takahashi

Correspondence to: kkuroda@staff.kanazawa-u.ac.jp

Supporting Figures

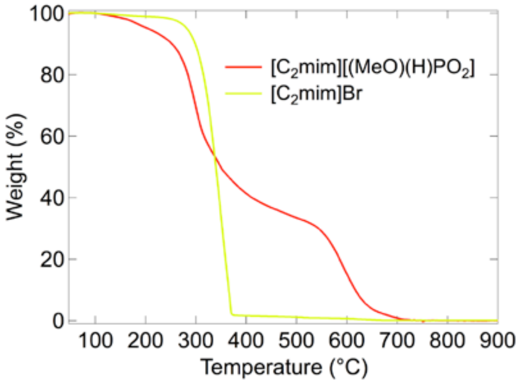

Fig. S1 TGA curves of [C_2mim][(MeO)(H)PO_2] which were used in this study under air condition.

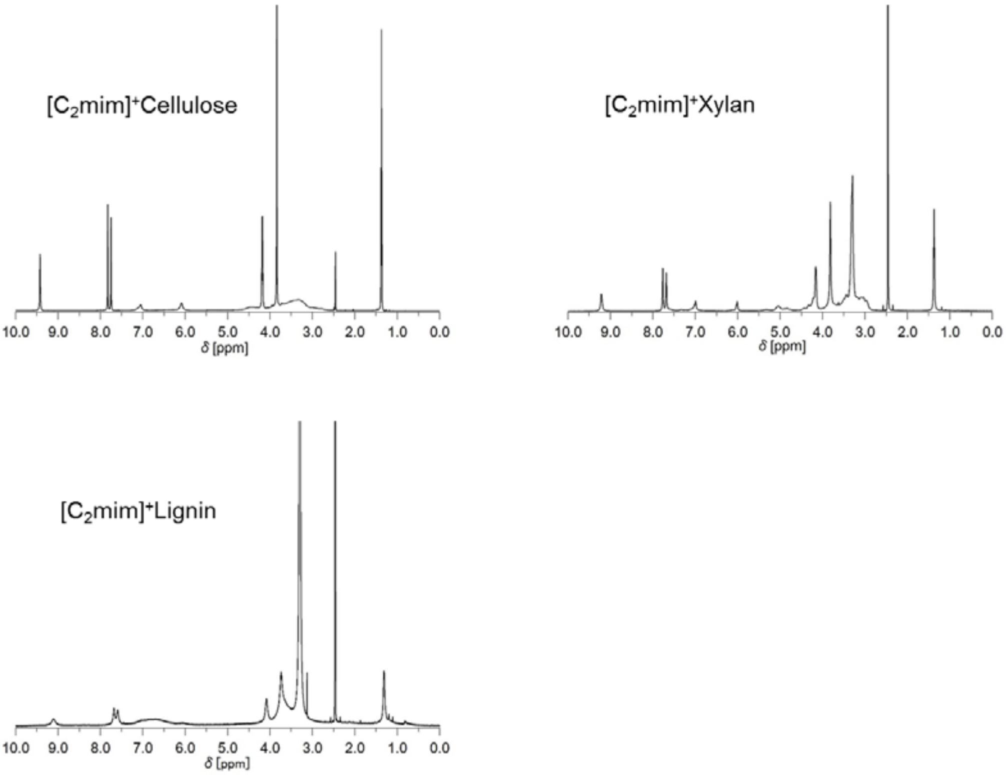

Fig. S2 ^{1}H NMR spectra of $[C_2mim]^+$cellulose, $[C_2mim]^+$xylan and $[C_2mim]^+$lignin in DMSO-d_6.

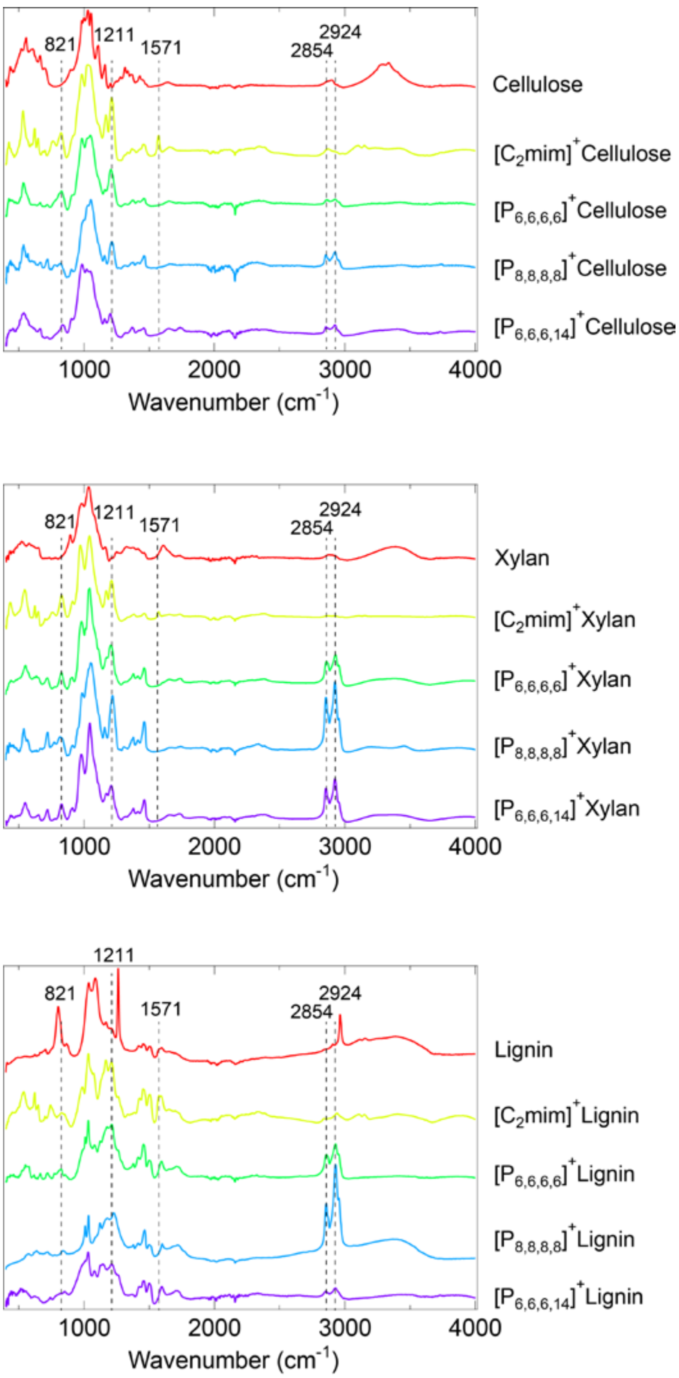

Fig. S3 FT-IR spectra of the underivatised and derivitised cellulose, xylan, and lignin.

The peaks derived from the P-O-C bond at 821 cm^{-1}, P=O bond at 1211 cm^{-1}, and C=N bond at 1571 cm^{-1} were detected in $[C_2mim]^+$cellulose, $[C_2mim]^+$xylan and $[C_2mim]^+$lignin. The peaks derived from the C-H bond of phosphonium cation at 2854 and 2924 cm^{-1} were also detected in the spectrum of phosohonium-type derivatives. In the case of lignin derivatives, the signals are not strong due to the low derivatisation ratio.

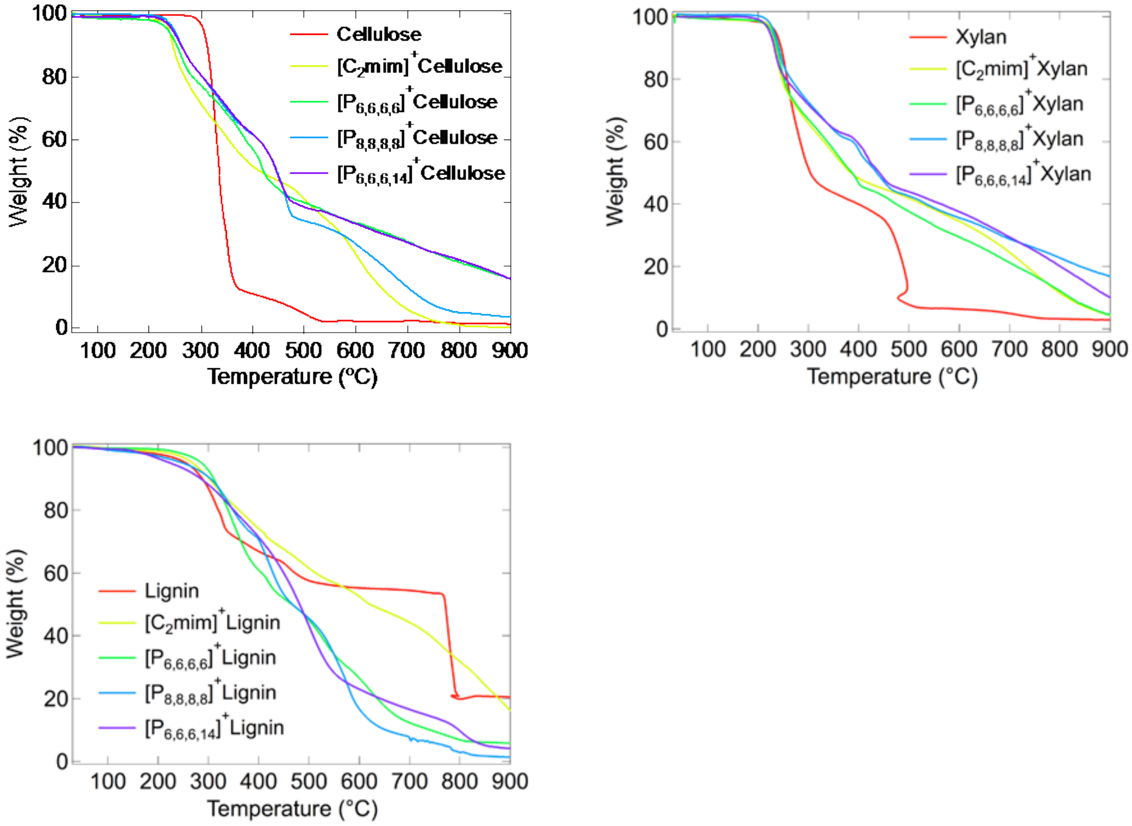

Fig. S4 TGA curves of the underivatised and derivitised cellulose, xylan, and lignin measured under air condition.

TG signals sometimes behaved abnormally (for example in the case of underivatised xylan) and the abnormal behaviour is attributed to the combustion of the samples because the samples were measured under air condition.

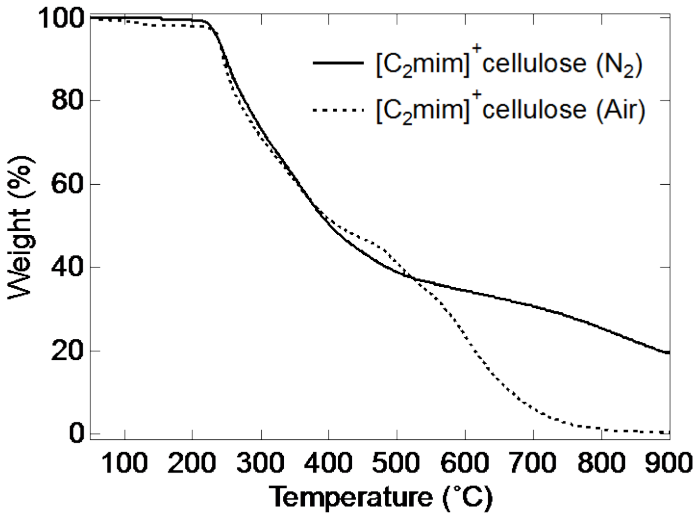

Fig. S5 TGA curves of $[C_2mim]^+$cellulose measured under air and nitrogen gas conditions.

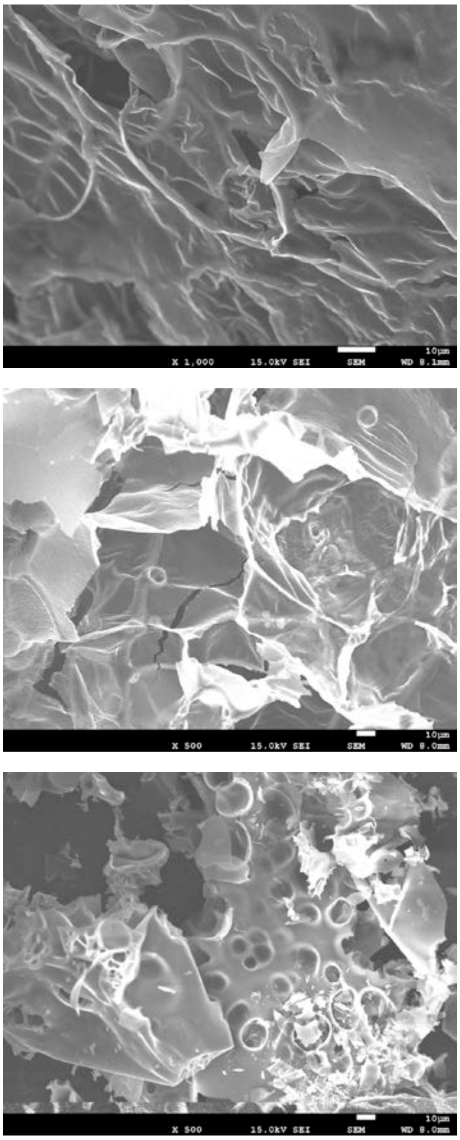

Fig. S6 SEM images of the char layers of $[C_2mim]^+$cellulose (top), $[C_2mim]^+$xylan (middle), $[C_2mim]^+$lignin (bottom).

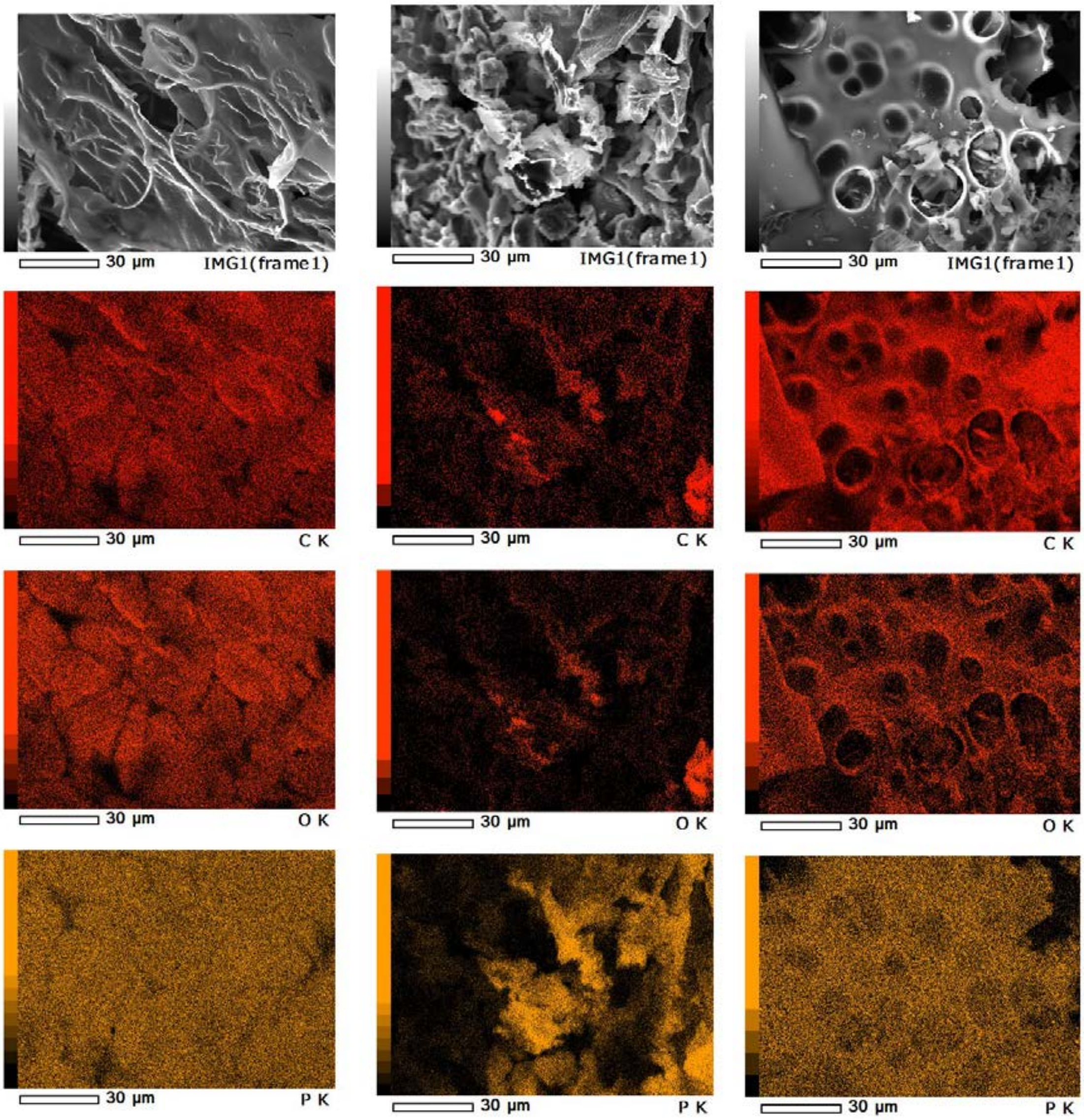

Fig. S7 SEM-EDX images of the char layers of $[C_2mim]^+$cellulose (top), $[C_2mim]^+$xylan (middle), $[C_2mim]^+$lignin (bottom).

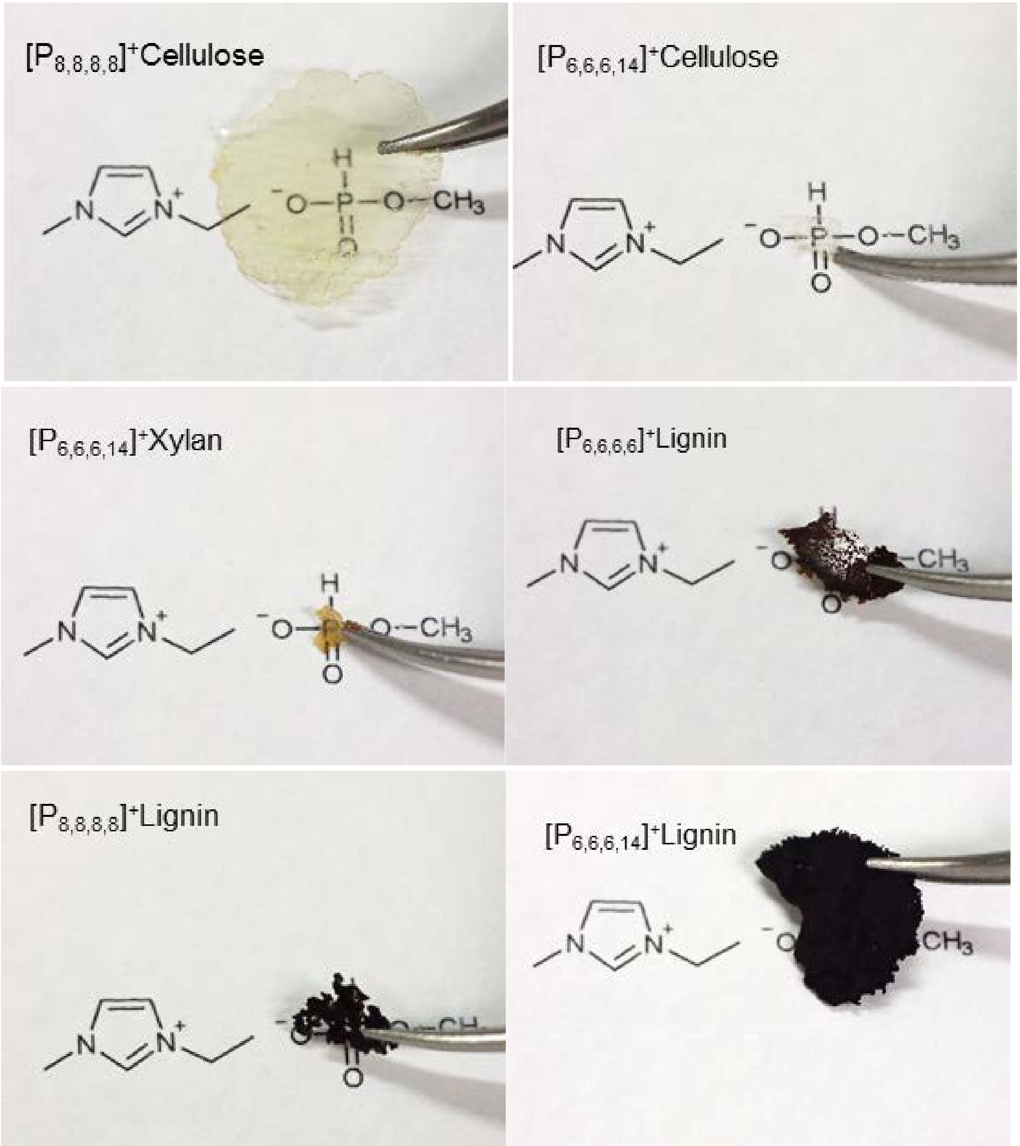

Fig. S8 Thin films of $[P_{8,8,8,8}]^+$cellulose, $[P_{6,6,6,14}]^+$cellulose, $[P_{6,6,6,14}]^+$xylan, $[P_{6,6,6,6}]^+$lignin, $[P_{8,8,8,8}]^+$lignin, and $[P_{6,6,6,14}]^+$lignin after hot pressing.

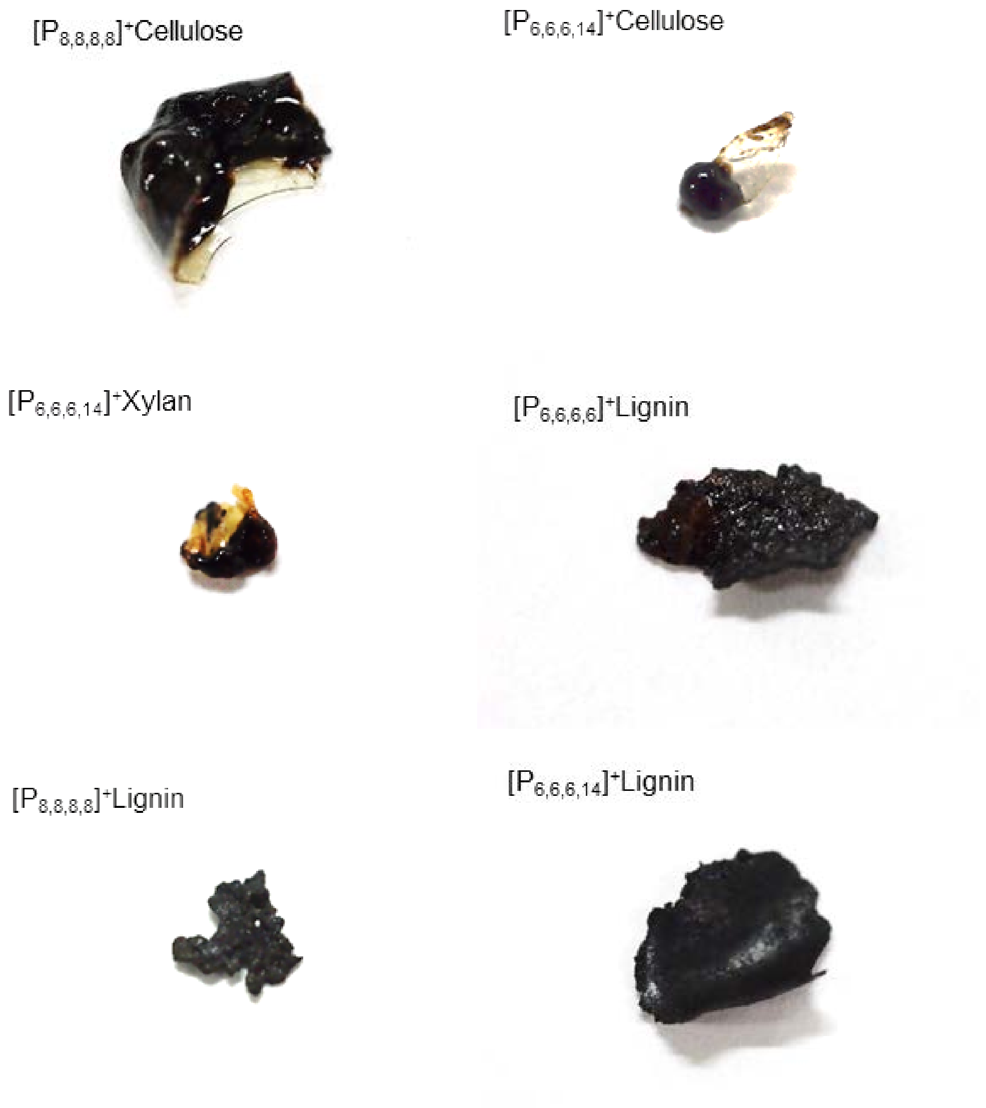

Fig. S9 Char formation of the thin films of $[P_{8,8,8,8}]^{+}$cellulose, $[P_{6,6,6,14}]^{+}$cellulose, $[P_{6,6,6,14}]^{+}$xylan, $[P_{6,6,6,6}]^{+}$lignin, $[P_{8,8,8,8}]^{+}$lignin, and $[P_{6,6,6,14}]^{+}$lignin after burning and extinguish the fire.

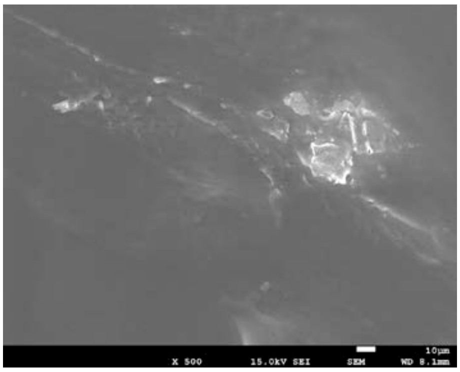

Fig. S10 A SEM image of the char layer of $[P_{8,8,8,8}]^{+}$cellulose.

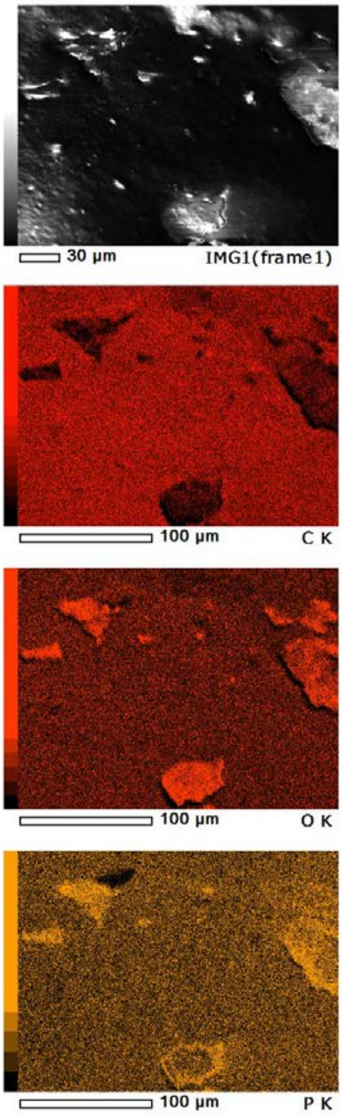

Fig. S11 A SEM-EDX image of the char layer of $[P_{8,8,8,8}]^{+}$cellulose.

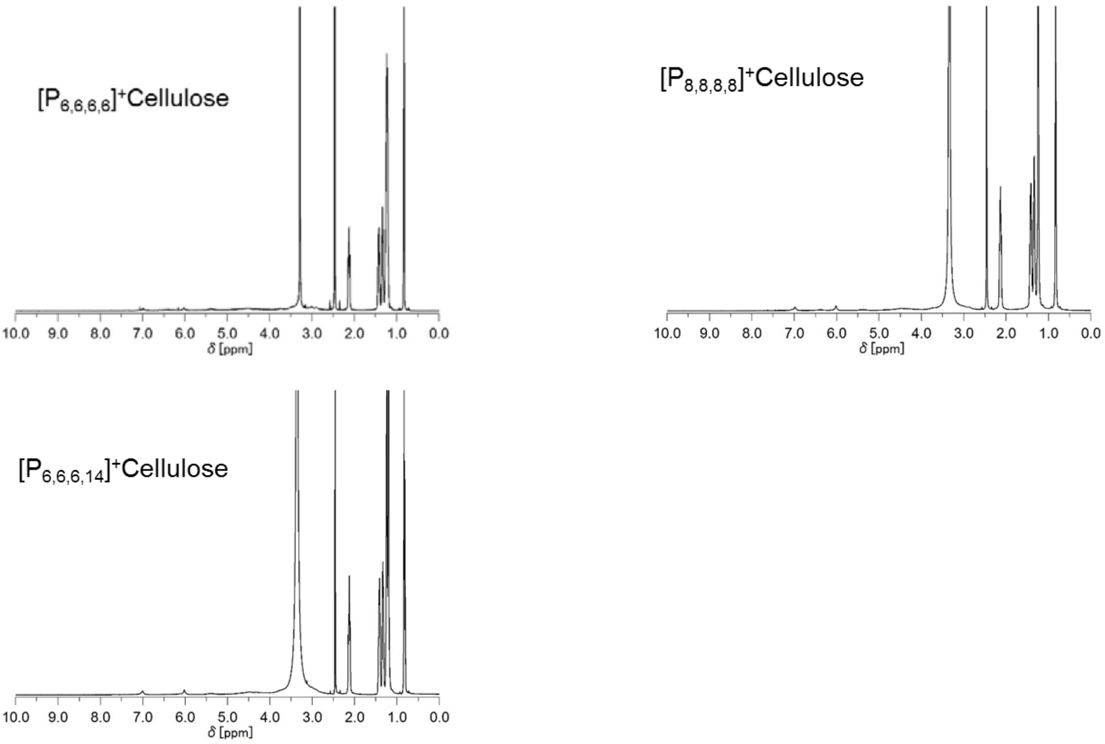

Fig. S12 ^{1}H NMR spectra of $[P_{6,6,6,6}]^{+}$, $[P_{8,8,8,8}]^{+}$, and $[P_{6,6,6,14}]^{+}$cellulose in DMSO-d_6. The signal at 3.4 ppm is water.

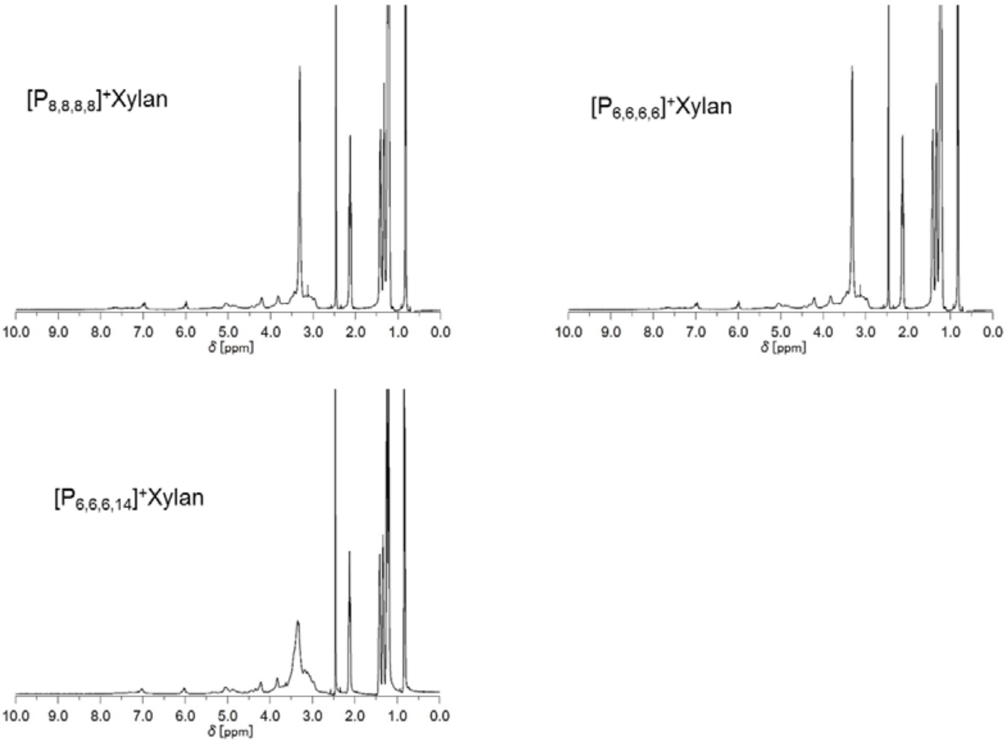

Fig. S13 ^{1}H NMR spectra of $[P_{6,6,6,6}]^+$, $[P_{8,8,8,8}]^+$, and $[P_{6,6,6,14}]^+$xylan in DMSO-d_6. The signal at 3.4 ppm is water.

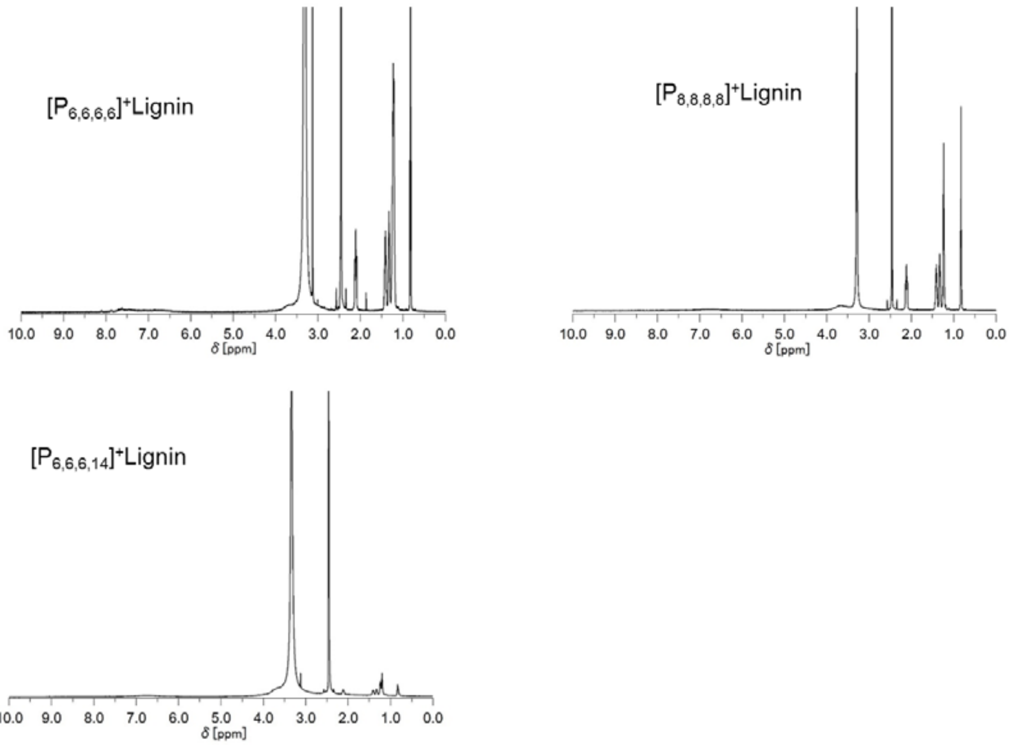

Fig. S14 ^{1}H NMR spectra of $[P_{6,6,6,6}]^+$, $[P_{8,8,8,8}]^+$, and $[P_{6,6,6,14}]^+$lignin in DMSO-d_6. The signal at 3.4 ppm is water.